Redox Biology 24 (2019) 101225

Contents lists available at ScienceDirect

Redox Biology

journal homepage: www.elsevier.com/locate/redox

Inhibition of SGK1 confers vulnerability to redox dysregulation in cervical cancer

Min Wang[a,1], Yijue Xue[a,1], Lanlin Shen[a,1], Pan Qin[b,1], Xiaolin Sang[a], Zhiwei Tao[a], Jingyan Yi[a], Jia Wang[c,***], Pixu Liu[a,**], Hailing Cheng[a,*]

[a] Cancer Institute, The Second Hospital of Dalian Medical University, Institute of Cancer Stem Cell, Dalian Medical University, Dalian, Liaoning, China
[b] Faculty of Electronic Information and Electrical Engineering, Dalian University of Technology, Dalian, Liaoning, China
[c] Department of Breast Surgery, Institute of Breast Disease, The Second Hospital of Dalian Medical University, Dalian, Liaoning, China

Keywords:
Cervical cancer
SGK1
NRF2
ROS
Melatonin

A B S T R A C T

Cervical cancer has poor prognosis and patients are often diagnosed at advanced stages of the disease with limited treatment options. There is thus an urgent need for the discovery of new therapeutic strategies in cervical cancer. The activation of SGK1 has been linked to the development of various cancer types but little is known about the role of SGK1 in cervical cancer and its potential as a therapeutic target. Here we report that SGK1 is an antioxidative factor that promotes survival of cervical cancer cells. Gene set enrichment analysis of RNA-Seq data reveals a strong inverse association between SGK1 and oxidative phosphorylation. Consistently, inhibition of SGK1 via siRNA or pharmacological inhibitor GSK650394 induces ROS and cytotoxicity upon H_2O_2 stress. Further analysis of clinical data associates SGK1 with gene expression signatures regulated by the antioxidant transcription factor NRF2 in cervical cancer. Mechanistically, SGK1 activation exerts antioxidant effect through induction of c-JUN-dependent NRF2 expression and activity. Importantly, we find that inhibition of SGK1 confers vulnerability to melatonin as a pro-oxidant, resulting in ROS over-accumulation and consequently enhanced cell cytotoxicity. We further demonstrate that combined use of GSK650394 and melatonin yields substantial regression of cervical tumors *in vivo*. This work opens new perspectives on the potential of SGK1 inhibitors as sensitizing agents to enable the design of therapeutically redox-modulating strategies against cervical cancer.

1. Introduction

Cervical cancer remains one of the most lethal gynecological malignancies worldwide. Late-stage or recurrent cervical cancers are generally considered incurable, and treatment options are very limited [1,2]. There is thus an urgent need to develop novel effective therapeutic strategies for advanced cervical cancer.

Manipulating reactive oxygen species (ROS) levels by redox modulation to selectively kill cancer cells while sparing normal cells has been a feasible and attractive approach to achieve therapeutic activity [3,4]. Redox adaptation plays a crucial role in malignant transformation, metastasis, and drug resistance. As an adaptive response to intrinsic ROS stress, cancer cells have developed upregulated antioxidant capacity to maintain redox homeostasis through activating ROS-sensitive transcription factors such as NRF2 (NFE2L2), leading to an elevated expression of antioxidant molecules [5–7]. NRF2 is a master regulator of ROS homeostasis involved in the pathogenesis of a variety of diseases [6,8–10]. Mounting evidence has suggested an oncogenic role of NRF2 and its association with chemotherapy resistance in a variety of malignant tumors including cervical cancer [5,6,8,11,12]. Notably, a recent study by proteomic analyses of secretomes of cervical cancer cell lines indicated an association of impaired

Abbreviations: SGK1, the Serum and Glucocorticoid-induced Kinase 1; ROS, Reactive Oxygen Species; H_2O_2, hydrogen peroxide; NRF2, Nuclear factor (erythroid-derived 2)-like 2; KEAP1, Kelch-like ECH-associated protein 1; PARP, Poly (ADP-ribose) polymerase; γH2AX, phosphorylated histone H2AX at Serine 139; TCGA, The Cancer Genome Atlas; GSH, Glutathione; IHC, Immunohistochemistry; qRT-PCR, Quantitative Reverse Transcription PCR; GSEA, Gene Set Enrichment Analysis; DFCH-DA, 2′, 7′-dichlorofluorescin diacetate; CCK8, Cell Counting Kit-8; ARE, Antioxidant Response Element

* Corresponding author. The Second Hospital of Dalian Medical University, 467 Zhongshan Road, Dalian, Liaoning, China.
** Corresponding author. Institute of Cancer Stem Cell, Dalian Medical University, 9 West Lv Shun Nan Road, Dalian, Liaoning, China.
*** Corresponding author. The Second Hospital of Dalian Medical University, 467 Zhongshan Road, Dalian, Liaoning, China.
E-mail addresses: wangjia77@hotmail.com (J. Wang), pixu_liu@dmu.edu.cn (P. Liu), hailingcheng_dmu@163.com (H. Cheng).
[1] These authors contributed equally.

https://doi.org/10.1016/j.redox.2019.101225
Received 15 February 2019; Received in revised form 23 April 2019; Accepted 17 May 2019
Available online 20 May 2019

NRF2-mediated oxidative stress response with cervical carcinogenesis [13]. Somatic activating mutations in the *NRF2* gene have been found in up to 7% of cervical cancers [14,15], indicating that aberrant NRF2-mediated oxidative stress response may contribute to disease pathogenesis. In addition, methylation of NRF2-negative regulator KEAP1 that confers constitutive NRF2 activity has also been found in cervical cancer [11]. Considering the central role of NRF2 in maintaining redox balance, uncovering molecular mechanisms underlying the regulation of NRF2 activity is important for designing alternative treatment strategies for this disease.

Aberrant activation of the PI3K signaling pathway, mainly by genomic alterations in the *PIK3CA* or *PTEN* genes, has been frequently found in human cervical tumors [14–16], highlighting the therapeutic potential of targeting individual members of the PI3K pathway in this disease. The serum and glucocorticoid-induced kinase 1 (SGK1), a major downstream effector of PI3K signaling, belongs to the AGC family of serine/threonine kinases homologous to AKT [17,18]. High levels of SGK1 expression were found to confer resistance to PI3K/AKT inhibitors [18,19]. In addition, growing evidence has indicated that SGK1 is a stress-induced survival factor and that SGK1 expression is promptly induced under pathophysiological conditions such as growth factors, glucocorticoid, cytokines, and various cellular stresses such as heat shock, ultraviolet irradiation and oxidative stress. Meanwhile, SGK1 has been shown to promote tumor cell survival, reduce the chemotherapy-induced apoptosis, and confer drug resistance in multiple types of human malignancies [17,19,20]. For example, SGK1 promotes cytokine-stimulated growth of multiple myeloma [21], and androgen receptor-mediated growth of prostate cancer [22,23]. SGK1 induced by glucocorticoid or H_2O_2 inhibits paclitaxel or doxorubicin-induced apoptosis in breast cancer cells [24–26], and SGK1 also confers cisplatin resistance in ovarian cancer cells [27]. It is worth noting that multiple lines of evidence indicate that SGK1 promotes the growth and survival of colorectal cancer both *in vitro* and *in vivo* [28–30]. Intriguingly, however, increased expression of SGK1 has been recently shown to promote colon cancer cell differentiation and restrain metastasis [31], thus adding another layer of complexity to the understanding of SGK1's actions in cancer. Thus far, a functional role of SGK1 in cervical cancer has not been established.

In the current study, we sought to investigate the biological role of SGK1 in cervical cancer and its potential as a therapeutic target. We report that SGK1 is an anti-oxidative factor that promotes survival of cervical cancer cells through modulating the c-JUN/NRF2 signaling axis. Importantly, we demonstrate that inhibition of SGK1 confers vulnerability to redox dysregulation, and that melatonin as a pro-oxidant potentiates the cytotoxic effect of SGK1 inhibition in cervical cancer both *in vitro* and *in vivo*.

2. Materials and methods

2.1. Cell culture and reagents

All cell lines used in this study were obtained from the American Type Culture Collection (ATCC) in 2015. The cell lines were authenticated through short tandem repeat analysis at the beginning of this study. Cells were maintained in culture medium (CaSki in RPMI-1640 medium, ME180 in mcCoy's 5A (modified) medium, SiHa in MEM/EBSS medium, HeLa and 293T cells in DMEM medium) supplemented with 10% fetal bovine serum (Biological Industries, Israel) and 100 units/ml penicillin/streptomycin (Gibco, USA) in a humidified incubator at 5% CO_2 and 37 °C. Cells were tested periodically for mycoplasma contamination. All cell culture media were purchased from Invitrogen (USA). Melatonin was obtained from MedChemExpress (MCE, China) and GSK650394 from Biochempartner (Shanghai, China). H_2O_2 and GSH were obtained from Sigma (USA).

To construct pWzl-HA-SGK1, human full-length cDNA for SGK1 was amplified and cloned into pWzl-blast (kindly provided by Dr. Jean Zhao at Dana-Farber Cancer Institute, USA). The kinase-inactive mutant SGK1 K127 M and the constitutively active mutant SGK1 S422D were generated using PCR based site-directed mutagenesis (TOYOBO, USA). The sequences of plasmids were verified by sequencing.

2.2. siRNA transfection

Cells were seeded in 6-well plates and transfected with on-target or non-target (siControl) siRNAs using Lipofectamine 2000 (Invitrogen, USA) according to the manufacturer's instruction. Cells were harvested at 72 h post transfection and subjected to further analyses. The siRNAs were custom synthesized from GenePharma (Suzhou, China), and the sequence information was listed as follows:

si*SGK1*#1-sense: 5′-GCCAAUAACUCCUAUGCAUTT-3′

si*SGK1*#1-anti-sense: 5′-AUGCAUAGGAGUUAUUGGCTT-3′

si*SGK1*#2-sense: 5′-CCGCCAGCUGACAGGACAUTT-3′

si*SGK1*#2-anti-sense: 5′-AUGUCCUGUCAGCUGGCGGTT-3′

si*c-JUN*-sense: 5′-GAAAGUCAUGAACCACGUUTT-3′

si*c-JUN*-anti-sense: 5′-AACGUGGUUCAUGACUUUCTT-3′

si*JUNB*-sense: 5′-CACCUCCCGUUUACACCAATT-3′

si*JUNB*-anti-sense: 5′-UUGGUGUAAACGGGAGGUGTT-3′

si*NRF2*-sense: 5′-GCUUUUGGCGCAGACAUUCTT-3′

si*NRF2*-anti-sense: 5′-GAAUGUCUGCGCCAAAAGCTG-3′

2.3. Long-term cell viability assay

Cells were plated on 96-well plates and treated with or without drugs for days as indicated. The culture medium was replaced with freshly prepared drug-containing medium every other day. The cells were fixed and stained with 0.5% crystal violet solution, washed and dried. Bound crystal violet was resolved by 50% acetic acid solution. The optical absorbance (OD) of bound crystal violet was measured at 590 nm using the Multi-functional microplate reader Enspire230 (PerkinElmer, USA).

2.4. CCK8 assay

The CCK-8 assay (Dojindo Molecular Technologies, Japan) was carried out according to the manufacturer's guidelines. The optical density (OD) was measured at 450 nm by an xMark Microplate Spectrophotometer (Bio-Rad, USA).

2.5. RNA sequencing analysis

RNA was isolated from siSGK1-transfected ME180 or siControl cells using TRIzol Reagent (Invitrogen). RNA-Seq was performed by the Novogene Corporation (Beijing, China). The sequencing libraries were created using NEBNext® UltraTM RNA Library Prep Kit for Illumina® (NEB, USA) according to the manufacturer's instructions. Gene set enrichment analysis (GSEA) was performed to identify the molecular pathways correlated to SGK1 knockdown in ME180 cells by the JAVA program (http://software.broadinstitute.org/gsea/index.jsp) using Molecular Signatures Database (MSigDB). 1000 permutations were conducted, and gene sets with false discovery rate (FDR) ≤ 0.05 and nominal p-values ≤ 0.01 were considered significantly enriched. The RNA-seq dataset was deposited to the Gene Expression Omnibus (GEO) with accession number GSE130449.

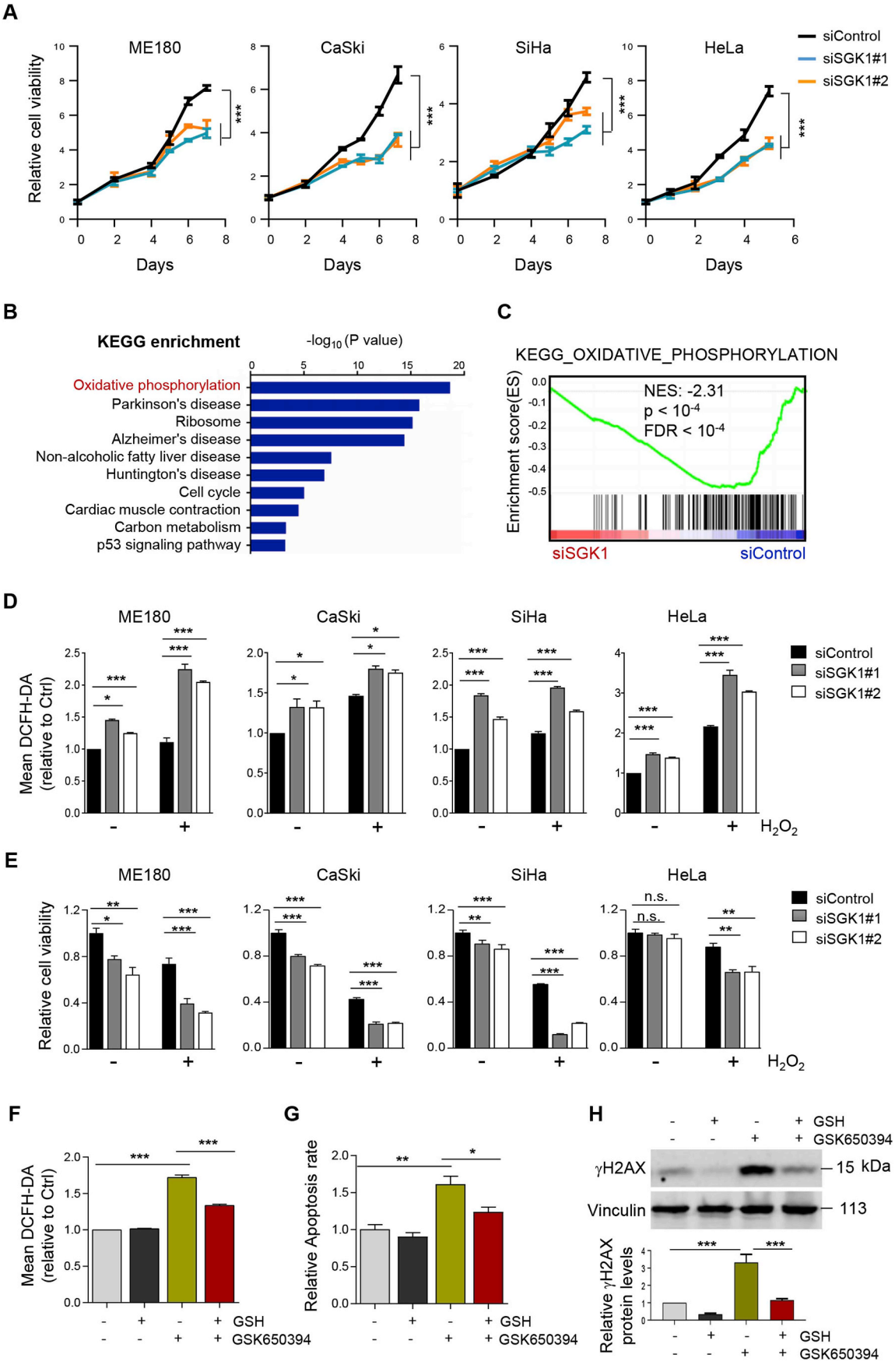

(caption on next page)

Fig. 1. SGK1 exhibits anti-oxidant activity in cervical cancer cells. (A) Long-term cell viability of siSGK1-transfected cervical cancer cells was measured by crystal violet assay. (B) Analysis of RNA-Seq data reveals top ten KEGG pathways associated with SGK1 expression in ME180 cells. (C) GSEA of oxidative phosphorylation signature in siSGK1-transfected ME180 cells versus control cells. Normalized enrichment score (NES) and False discovery rate (FDR) q value of the correlation are shown. (D) Flow cytometric analysis of ROS levels, as indicated by DCFH-DA fluorescence, in siSGK1-transfected cervical cancer cells treated with or without 500 μM H_2O_2 for 1 h. Data are shown as means ± S.D. for three independent experiments. (E) Cell viability was measured by using CCK8 assay for cells treated as in (D). (F) Flow cytometric analysis of ROS levels in ME180 cells treated with GSK650394 (5 μM) and/or GSH (1 mM) for 24 h. Data are shown as means ± S.D. for three independent experiments. (G) Apoptosis levels as revealed by Annexin V/PI staining assays were determined in cells treated as in (F). Quantification for three independent experiments is shown. (H) Western blot analysis of proteins in cells treated as in (F). Vinculin was used as a loading control. The quantification of protein abundance is shown. n. s., not significant. *p ≤ 0.05, **p ≤ 0.01, ***p ≤ 0.001 (Student's *t*-test). (For interpretation of the references to color in this figure legend, the reader is referred to the Web version of this article.)

2.6. Quantitative reverse transcription PCR (qRT-PCR)

Total RNA was isolated using TRIzol Reagent (Invitrogen, USA) according to the manufacturer's instructions. For gene expression analysis, reverse transcription reaction was performed using the cDNA synthesis kit (TaKaRa, Japan), and the gene expression levels were analyzed by qRT-PCR using SYBR Select Master Mix (Applied Biosystems, USA) in the Mx3005P Real-Time PCR system (Aglient, USA). The relative expression levels of target genes were calculated using the delta-delta-Ct (ΔΔCT) method (expressed as $2^{-\Delta\Delta CT}$) and normalized to *ACTB* as an endogenous control. Primers used for gene expression are shown as follows:

NRF2: Fw 5′-CACATCCAGTCAGAAACCAGTGG-3′

Rv 5′-GGAATGTCTGCGCCAAAAGCTG-3′

AKR1C2: Fw 5′-TCTGCAACCAGGTGGAATGTCAT-3′

Rv 5′-CTGGGGTTCGCTTGTGCTTTT-3′

GPX2: Fw 5′-TTTGGACATCAGGAGAACTGTC-3′

Rv 5′-AGACAGGATGCTCGTTCTGC-3′

GPX4: Fw 5′-AAGATCCAACCCAAGGGCAA-3′

Rv 5′-GCAGCCGTTCTTGTCGATG-3′

TXN: Fw 5′-GATGTGGATGACTGTCAGGATG-3′

Rv 5′-TTCACCCACCTTTTGTCCCTT-3′

GLRX: Fw 5′-TTGGAGCTCTGCAGTAACCAC-3′

Rv 5′-CATCCACCAGAAGTGCTGTCA-3′

PRDX2: Fw 5′-GTCCAGGCCTTCCAGTACAC-3′

Rv 5′-TGTCATCCACGTTGGGCTTA-3′

c-JUN: Fw 5′-CCAAGAACTCGGACCTCCTC-3′

Rv 5′-CCCGTTGCTGGACTGGATTA-3′

JUNB: Fw 5′-ACCTCCCGTTTACACCAACC-3′

Rv 5′-TGTGGGAGGTAGCTGATGGT-3′

ACTB: Fw 5′-CATGTACGTTGCTATCCAGGC-3′

Rv 5′-CTCCTTAATGTCACGCACGAT-3′

2.7. Cellular ROS detection

Cellular ROS levels were measured using Reactive Oxygen Species (ROS) Detection Reagents (ThermoFischer Scientific, C2938) according to the manufacturer's protocol. Briefly, cells were seeded in 6-well plates and cultured with or without drug treatments as indicated. Cells were then harvested, stained with 5 μM ROS reagent (2′, 7′dichlorofluorescein diacetate, DCFH-DA) for 1 h at 37 °C, and analyzed on BD FACSCanto™II (BD Biosciences, USA).

2.8. Western blot analysis

Cell lysates were prepared using RIPA buffer supplemented with protease/phosphatase inhibitors (Roche, USA). Western blot experiment was conducted as described previously [32]. The following primary antibodies were used: SGK1 (Cell signaling technology, CST 12103S, 1:1000), *p*-SGK1 (Abcam ab55281, 1:2000), cleaved PARP (CST 9541S, 1:1000), c-JUN (CST 9165S, 1:1000), p-c-JUN (CST 3270S, 1:1000), JUNB (CST 3753S, 1:1000), *p*-GSK3α/β (CST 9331S, 1:1000), GSK3β (CST 12456S, 1:1000), γH2AX (CST 2577S, 1:1000), NRF2 (Abcam ab62352, 1:1000), and Vinculin (Sigma Aldrich V9131, 1:10000). Western blots were imaged using Odyssey (LI-COR Biosciences, USA).

2.9. Flow cytometric analysis

Apoptosis assay was performed by using the Annexin V/PI Apoptosis Detection kit (Dojindo Molecular Techonologies, AD10, Japan) according to the manufacturer's protocol. Briefly, cells were seeded on 6-well plates and drug treated. Cells were then harvested, washed with 1x staining buffer and stained with Annexin V/Propidium Iodide solution in dark for 15min. Stained cells were analyzed on BD FACSCanto™II (BD Biosciences, USA).

2.10. Three-dimensional spheroid assay

Three-dimensional (3D) sphere culture was performed as previously described [33]. Briefly, cervical cancer cells were seeded on 96-well plates coated with Matrigel (BD Biosciences, USA) plus 50% of medium without serum. Cells were grown in culture medium supplemented with 2% FBS and 2% Matrigel with or without indicated drug treatments. Medium was refreshed every 3 days. 3D structures were imaged by inverted phase contrast microscope (Leica Microsystems, Germany) and scored according to 3D structure integrity. Over 100 colonies were scored for each group.

2.11. Histology and immunohistochemical staining

Tumors were fixed in formalin overnight before paraffin embedding. Paraffin blocks were sectioned and stained with H&E. For histological analysis, sectioned paraffin blocks were stained with Hematoxylin and Eosin (H&E). For immunohistochemical staining, the following primary antibodies were used: γH2AX (CST 2577S, 1:800), Ki67 (Abcam ab15580, 1:800), NRF2 (Proteintech 16396-1-AP, 1:300) and *p*-SGK1 (Abcam ab55281, 1:2000). For each tumor sample, 3–5 random 40 × fields were scored. Protein levels were quantified using Image Pro Plus software.

2.12. Clinical data analysis

The data of TCGA_Cervical were downloaded from cervix uteri (CESC) in The Cancer Genome Atlas data portal (https://portal.gdc.cancer.gov/) [15], and Halle_ cervical cancer from GSE36562 (http://www.ncbi.nlm.nih.gov/geo/) [34]. We use the genes in “SINGH_NFE2L2_TARGETS”, “NRF2_Q4” and “NFE2L2. V2” gene sets from

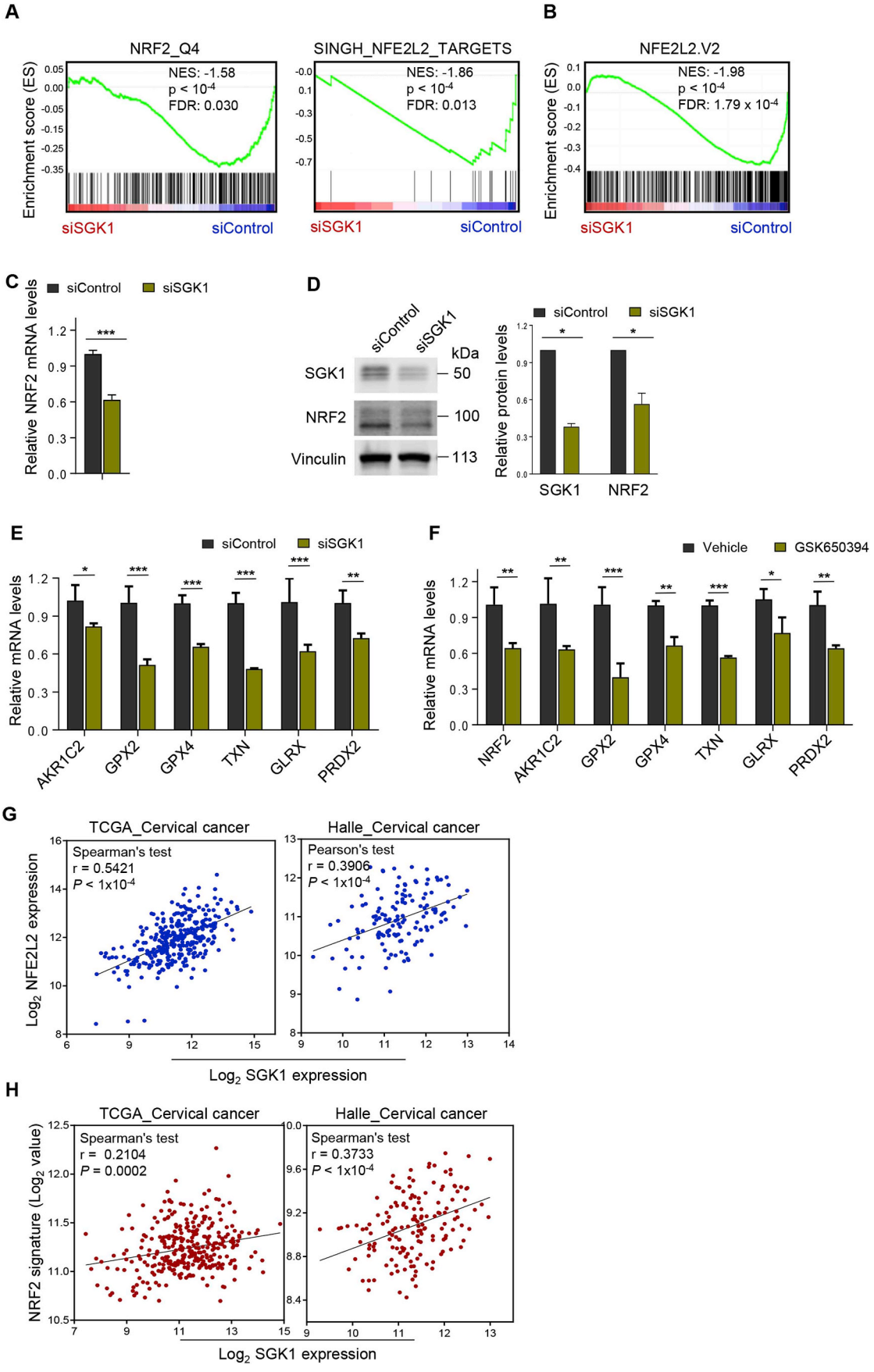

(caption on next page)

Fig. 2. SGK1 expression correlates with NRF2 gene signatures in cervical cancer cells. (A–B) Gene set enrichment analysis of NRF2 gene signatures in siSGK1#1 transfected ME180 cells versus control cells. NES and FDR q values of the correlation are shown. (C) Quantitative RT-PCR analysis of NRF2 mRNA levels in siSGK1#1 transfected ME180 or control cells. *ACTB* was used as an endogenous control. Mean ± S.D. for three independent experiments are shown. *p ≤ 0.05, **p ≤ 0.01, ***p ≤ 0.001 (Student's *t*-test). (D) Western blot analysis of NRF2 protein levels in cells as in (C). Vinculin was used as a loading control. The quantification of protein abundance is shown. (E) Quantitative RT-PCR analysis of the mRNA levels of NRF2 transcriptional targets in siSGK1#1-transfected ME180 or control cells. (F) Quantitative RT-PCR analysis of the mRNA levels of NRF2 and its transcriptional targets in ME180 cells treated with GSK650394 or vehicle. GSK650394, 2.5 μM, 48 h. (G) The gene expression levels of SGK1 and NFE2L2 (NRF2) were measured in the TCGA [15] and GSE36562 [34] datasets. The gene expression is reported as $\log_2$ values and plotted as NFE2L2 gene expression over SGK1 gene expression. Each dot represents an individual sample of human cervical carcinoma (n = 309 for TCGA_cervical cancer; n = 135 for Halle_cervical cancer). (H) SGK1 gene expression is plotted against the NRF2 signature for TCGA and GSE36562 datasets. Correlation values and *P* values were determined as indicated.

molecular signatures database to serve as NRF2 signature [35]. For the datasets TCGA and GSE36562, the NRF2 signature centroid was calculated by determining the average expression values with respect to the NRF2 signature genes and three outliers in TCGA dataset were eliminated using interquartile range. The target genes were plotted against the NRF2 signature centroid. The correlation values and the *p*-values were determined using the Pearson's correlation or Spearman's correlation based on whether the data follow bivariate normal distribution and are homoscedastic. The analysis of clinical data was performed with GraphPad Prism 6.0 (GraphPad Software Inc, San Diego, CA, USA). In the graphs, each dot represents an individual sample.

2.13. In vivo mouse xenograft study

All the animal experiments were carried out in accordance with the approval of the Animal Research Committee of Dalian Medical University. Eight-week-old female nude mice (Beijing Vital River Laboratory Animal Technology Co., Ltd, China) were maintained in a pathogen-free environment. Approximately 7×10^6 ME180 cells mixed with Matrigel (BD Biosciences) in a total volume of 0.1ml/ mouse were inoculated into nude mice subcutaneously. Drug treatment started when tumors reached an average volume of 100 mm^3. The mice were randomly divided into four groups with roughly equal mean tumor volume and administered with vehicle, GSK650394, melatonin, or the combination daily for consecutive 28 days. The tumor volumes were measured every other day with calipers and were calculated according to the following formula: tumor volume = (length × $width^2$)/2.

2.14. Statistical analysis

The unpaired two-sided t-tests and the one-way ANOVA with Tukey's multiple-comparisons tests were performed using GraphPad Prism software for analysis of the data obtained *in vitro* and *in vivo*, respectively. *P*-value < 0.05 was considered as statistical significance.

3. Results

3.1. Inhibition of SGK1 results in elevated ROS levels in cervical cancer cells

To interrogate the biological role of SGK1 in cervical cancer, we knocked down SGK1 in four cervical cancer cell lines, ME180, CaSki, SiHa and HeLa, via siRNA (Supplementary Fig. 1A). The results revealed that SGK1 knockdown via siRNA significantly attenuated the cell growth as determined by long-term cell viability assays (Fig. 1A). To understand the molecular consequences of SGK1 knockdown, we compared the transcriptomes of SGK1-knockdown ME180 cells with the control cells by RNA sequencing (RNA-Seq) and identified oxidative phosphorylation as the most significantly enriched pathway (Fig. 1B). Gene set enrichment analysis (GSEA) indicated that the oxidative phosphorylation gene signature was negatively enriched in SGK1-knockdown cells (Fig. 1C). These findings, for the first time, point to a potential role of SGK1 in regulating redox homeostasis in cervical cancer cells.

We then extended these findings to investigate the effect of SGK1 inhibition on ROS levels. The basal ROS levels were discernably higher in SGK1-knockdown cervical cancer cells (Fig. 1D). Upon hydrogen peroxide (H_2O_2)-stress, SGK1 knockdown resulted in significantly elevated ROS levels compared with the control cells (Fig. 1D), and a concomitant sensitization to H_2O_2-induced cell death (Fig. 1E). Consistently, restoring SGK1 expression abolished SGK1 knockdown-induced ROS and cytotoxicity in H_2O_2-stressed ME180 and CaSki cells (Supplementary Fig. 1B-D). Together, these data suggest that SGK1 may exhibit an anti-oxidant activity in cervical cancer.

Next, we tested the impact of GSK650394, a selective SGK1 inhibitor [23,30], on ROS homeostasis. In agreement with the effect of siRNA-mediated SGK1 knockdown, GSK650394 also significantly reduced cell viability (Supplementary Fig. 2). Importantly, the sensitivity to GSK650394 in ME180 cells was proportional to the augmented ROS levels and correlated with an induction of apoptosis as well as oxidative stress-induced DNA damage as indicated by γH2AX signals (Fig. 1F–H). The ROS scavenger reduced glutathione (GSH) reversed the effects of GSK653094 on ROS production, cytotoxicity and survival (Fig. 1F–H). Collectively, these data suggest that SGK1 exhibits anti-ROS activity necessary to promote the survival of cervical cancer cells.

3.2. SGK1 regulates NRF2 expression and activity in cervical cancer cells

To understand how SGK1 confers an antioxidative effect, we investigated whether SGK1 knockdown in ME180 cervical cancer cells is accompanied by gene-expression changes associated with specific anti-oxidant transcriptional factors. Strikingly, GSEA revealed a highly significant association of SGK1 expression with the gene sets controlled by human NRF2, a master anti-oxidant transcription factor (Fig. 2A). It is worth noting that a strong and significant association between SGK1 expression and mouse Nrf2 gene signature was also observed (Fig. 2B) [36], suggesting a conserved functional role of SGK1 in redox regulation. Furthermore, knockdown of SGK1 resulted in significant reduction in NRF2 mRNA and protein levels (Fig. 2C and D). Concordantly, the mRNA levels of NRF2 transcriptional targets, including *AKR1C2, GPX2, GPX4, TXN, GLRX and PRDX2*, were downregulated in SGK1-knockdown ME180 cells compared with the control cells (Fig. 2E) [7]. Consistently, SGK1 inhibitor GSK650394 treatment resulted in similar effects (Fig. 2F). These data pointed to a potential role of SGK1 in regulation of NRF2 expression and activity in cervical cancer cells. In support of these findings, analyses of TCGA_cervix uteri [15] and Halle et al. [34] cervical cancer cohorts yielded a significant association between the expression of *SGK1* and *NRF2* (Fig. 2G). We further investigated whether SGK1 expression functionally correlates with NRF2-driven transcription in these two cohorts. Indeed, we observed a moderate but significant correlation between SGK1 expression and NRF2-regulated gene expression signatures in both data sets (Fig. 2H). These findings, together with the potential role of SGK1 as an anti-oxidative factor (Fig. 1), prompted us to investigate whether SGK1 functionally regulates NRF2 expression.

We went on to investigate the functional importance of SGK1 kinase activity on NRF2 expression. First, we stably expressed constitutively activated (CA) mutant SGK1 S422D or kinase-dead (KD) mutant SGK1 K127 M in ME180 cervical cancer cells (Fig. 3A and Supplementary Fig. 3) [37]. Phosphorylation of GSK3β, a known substrate of SGK1

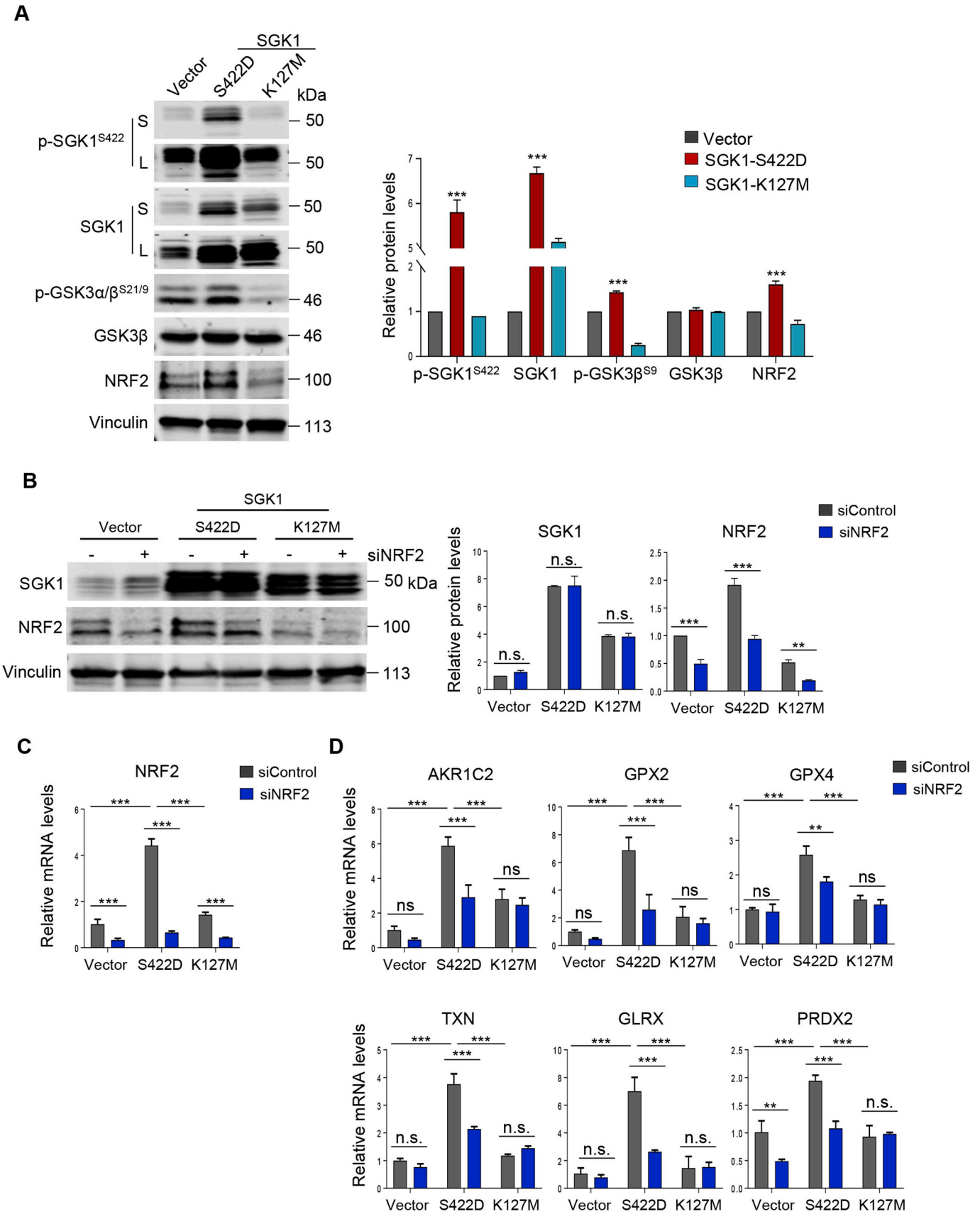

Fig. 3. SGK1 regulates NRF2 expression and activity in cervical cancer cells. (A) Western blot analysis of proteins as indicated in ME180 cells with ectopic overexpression of SGK1 S422D or K127 M. Vinculin was used as a loading control. The quantification of protein abundance is shown. (B) Western blot analysis of proteins as indicated in siNRF2-transfected ME180 cells with ectopic overexpression of SGK1 S422D or K127 M. Vinculin was used as a loading control. The quantification of protein abundance is shown. (C–D) Quantitative RT-PCR analysis of the mRNA levels of NRF2 and its transcriptional targets in cells as in (B). *ACTB* was used as an endogenous control. Mean ± S.D. for three independent experiments are shown. n. s., not significant. **p ≤ 0.01, ***p ≤ 0.001 (Student's *t*-test).

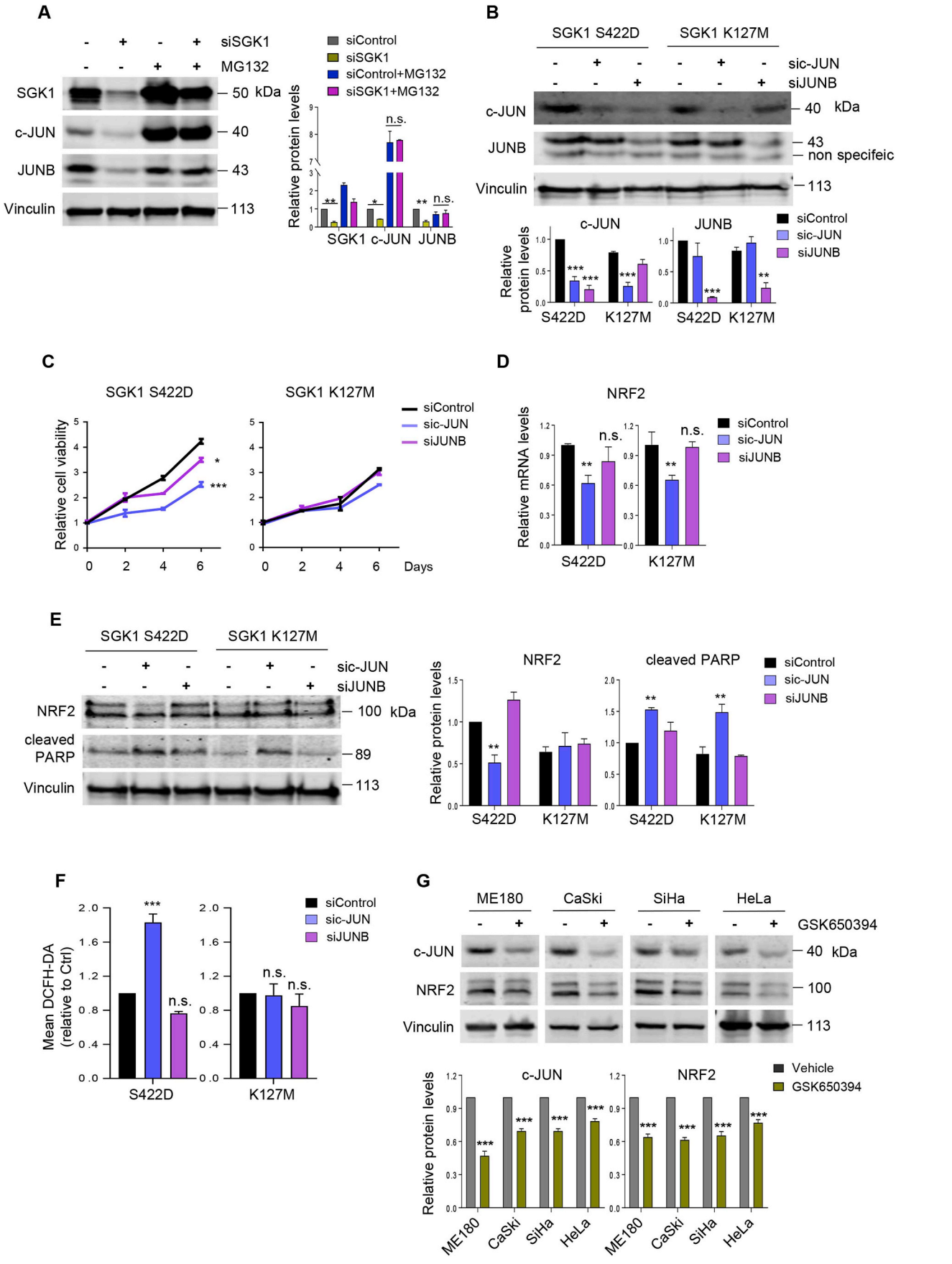

(caption on next page)

Fig. 4. SGK1 upregulates NRF2 expression in a c-JUN-dependent manner. (A) Western blot analysis of SGK1, c-JUN and JUNB proteins in siSGK1-transfected ME180 cells treated with or without MG132. Vinculin was used as a loading control. The quantification of protein abundance is shown. MG132, 10 μM, 6 h. (B) Western blot analysis of proteins as indicated in sic-JUN or siJUNB transfected ME180 cells with ectopic overexpression of SGK1 S422D or K127 M. Vinculin was used as a loading control. (C) Long-term cell viability was measured by crystal violet assay for cells as in (B). (D) Quantitative RT-PCR analysis of NRF2 mRNA levels in cells as in (B). *ACTB* was used as an endogenous control. Mean ± S.D. for three independent experiments are shown. (E) Western blot analysis of NRF2 and cleaved PARP in cells as in (B). Vinculin was used as a loading control. The quantification of protein abundance is shown. (F) Flow cytometric analysis of ROS levels in cells as in (B). (G) Western blot analysis of c-JUN and NRF2 proteins in cervical cancer cells treated with or without GSK650394. Vinculin was used as a loading control. The quantification of protein abundance is shown. n. s., not significant. *p ≤ 0.05, **p ≤ 0.01, ***p ≤ 0.001 (Student's *t*-test). . (For interpretation of the references to color in this figure legend, the reader is referred to the Web version of this article.)

[38], is significantly elevated in SGK1 kinase active (S422D) cells but diminished in SGK1 kinase dead (K127 M) cells (Fig. 3A), indicating that the SGK1 kinase activity is functional in S422D but absent in K127 M cells. While constitutive activation of SGK1 by ectopic overexpression of SGK1 S422D significantly induced the expression of NRF2 as well as its transcriptional target genes (*AKR1C2, GPX2, GPX4, TXN, GLRX and PRDX2*), inactivation of the SGK1 kinase by SGK1 K171 M had little effect (Fig. 3B–D). Furthermore, siRNA-mediated NRF2 silencing downregulated the expression of NRF2 transcriptional targets in SGK1 kinase active (S422D) ME180 cells but not in those SGK1 kinase dead cells (Fig. 3C and D). These results indicate that SGK1 may contribute to the induction of NRF2 expression and activity.

3.3. SGK1 exhibits anti-oxidant activity through modulating the c-JUN/NRF2 signaling axis in cervical cancer cells

We sought to further understand the molecular mechanism by which SGK1 regulates NRF2 expression. It has been reported that SGK1 regulates the stability of JUNB [39,40], a member of the family that also includes c-JUN and JUND [41]. Meanwhile, c-JUN has been demonstrated to bind to the promoter of NRF2 and regulate its expression [36]. We therefore considered the possibility that SGK1 may induce NRF2 expression in a c-JUN or JUNB-dependent manner. While knockdown of SGK1 reduced the levels of c-JUN and JUNB proteins in ME180 cells (Fig. 4A), it does not affect their mRNA levels (Supplementary Fig. 4A), suggesting that SGK1 may regulate the stability of c-JUN or JUNB proteins. Furthermore, we found that the protein abundance of c-JUN or JUNB is restored in SGK1 knockdown cells in the presence of MG132, a proteasome inhibitor (Fig. 4A), suggesting that SGK1 may negatively regulate the degradation of c-JUN or JUNB. Importantly, knockdown of c-JUN, and to a much lesser extent knockdown of JUNB, significantly reduced the viability of the SGK1 S422D cells (Fig. 4B and C, Supplementary Fig. 4B). In contrast, c-JUN or JUNB knockdown had little impact on the viability of the SGK1 kinase dead (K127 M) ME180 cells. Interestingly, knockdown of c-JUN, but not JUNB, resulted in reduced NRF2 expression, and consequently increased ROS levels and apoptosis in the SGK1 kinase active (S422D) cells (Fig. 4D–F). In contrast, similar effects were not seen in the SGK1 kinase dead cells. In addition, inactivation of SGK1 by GSK650394 also led to reduced abundance of NRF2 and c-JUN proteins (Fig. 4G). Together, these data indicate that SGK1 promotes the growth and survival of cervical cancer cells through upregulating the c-JUN/NRF2 signaling axis.

3.4. SGK1 inhibition combined with melatonin promotes ROS accumulation and cell cytotoxicity

Considering that SGK1 activation may upregulate the antioxidant capacity through NRF2 induction, we wondered whether this would allow cervical cancer cells to survive under higher oxidative stress. To test this, we selected melatonin as a ROS-inducer for its pro-oxidant activity as previously reported [42–44]. We first confirmed that melatonin induced ROS levels at mM range in cervical cancer cells (Supplementary Fig. 5A). Furthermore, we showed that while melatonin-induced ROS generation provoked a cytotoxic effect in ME180 cervical cancer cells, ectopic overexpression of the constitutively activated SGK1 mutant (S422D) significantly alleviated this effect (Supplementary Fig. 5B). These results therefore suggest SGK1 as an anti-oxidative factor that promotes the survival of cervical cancer cells under oxidative stress.

We next investigated whether inhibition of SGK1-mediated ROS elevation could be exploited as a vulnerability to melatonin-induced ROS insults. While SGK1 inhibitor GSK650394 augmented ROS levels, its combined use with melatonin resulted in a further ROS accumulation and a concomitant cytotoxicity (Fig. 5A and B). The response to the combination treatment was correlated with an inhibition of SGK1 signaling and an increase of DNA damage as evidenced by reduced phosphorylated SGK1 and increased γH2AX levels, respectively (Fig. 5C). Concordantly, combined use of GSK650394 and melatonin induced strong apoptosis as evidenced by cleaved PARP signal and Annexin V staining (Fig. 5C and D).

We also examined the responses of cervical cancer cells to GSK650394 and/or melatonin in 3D Matrigel cultures, a condition that mimics the natural microenvironment [45]. Combined treatment with GSK650394 and melatonin but not either single-treatment alone induced massive disintegration of the spheroids in all four cervical cancer cell lines (Fig. 5E). In addition, similar to the synergistic effect of melatonin with GSK650394, co-treatment with siRNA-mediated SGK1 inhibition resulted in significantly increased ROS levels, enhanced cell cytotoxicity and apoptotic cell death in ME180 and HeLa cervical cancer cells (Supplementary Fig. 6A-D). In line with the functional link between SGK1 and NRF2, combining siRNA-mediated NRF2 silencing and melatonin also yielded synergistic cytotoxicity in ME180 and CaSki cells (Supplementary Fig. 6E and F). Together, these data suggest that concomitant use of SGK1 inhibitor and melatonin as a pro-oxidant is effective in the treatment of cervical cancer cells.

3.5. The combination of GSK650394 and melatonin exhibits strong anti-tumor activity in vivo

To validate our *in vitro* findings, we next investigated whether melatonin potentiates the therapeutic effect of SGK1 inhibition on cervical cancer *in vivo*. While SGK1 inhibitor GSK650394 or melatonin alone slowed down the growth of ME180 human cervical tumor xenografts, the combination treatment resulted in dramatic tumor regression in all cases and even complete tumor remission in 33% (5/15) cases (Fig. 6A and B and Supplementary Fig. 7A and B). Tumors treated with GSK650394 alone or in combination with melatonin displayed significantly reduced phosphorylated SGK1 signals (Fig. 6C and Supplementary Fig. 7C), validating the target inhibition by SGK1 inhibitor. In addition, SGK1 inhibition by GSK650394 as single-agent, and to a more significant extent in combination with melatonin, strongly reduced the abundance of NRF2 protein (Fig. 6C). In line with the synergistic therapeutic effect, the combination treatment led to marked reduction of proliferation and induction of apoptosis as evidenced by Ki67 staining and cleaved PARP signals in tumors, respectively (Fig. 6C and D). Notably, mice treated with GSK650394 and melatonin in combination did not yield overt toxic effects, and mouse

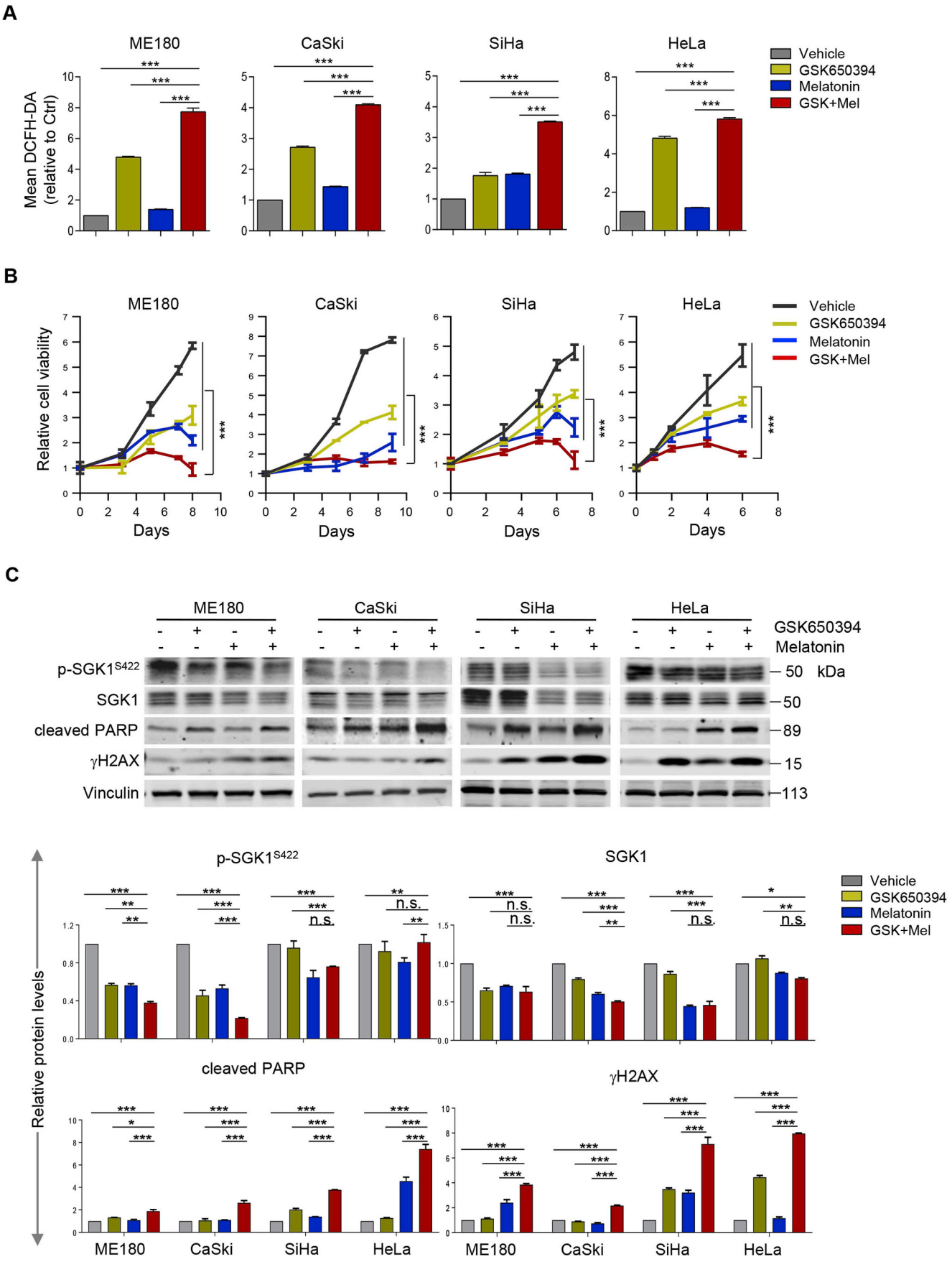

(caption on next page)

Fig. 5. SGK1 inhibition synergizes with melatonin to induce ROS-mediated apoptosis and cytotoxicity. (A) Flow cytometric analysis of ROS levels in cervical cancer cells treated with GSK650394 and melatonin, either alone or a combination of both for 48 h. Of note, CaSki and ME180 cells were treated with 2.5 μM GSK650394 and/or 1 mM melatonin; SiHa and HeLa cells were treated with 5 μM GSK650394 and/or 2 mM melatonin. (B) Long-term cell viability was measured by crystal violet assay for cells treated as in (A). (C) Western blot analysis of proteins in cells treated as in (A). Vinculin was used as a loading control. The quantification of protein abundance is shown. (D) Apoptosis levels in cells as in (A) were determined by Annexin V/PI staining assays. Quantification for three independent experiments is shown. (E) Cervical cancer cell lines were cultured in 3D Matrigel and treated with GSK650394 and melatonin, either alone or in combination. Representative images and Quantification of scored structures (intact, semi-disintegrated and disintegrated) are shown. Scale bars, 50 μm. n. s., not significant. *$p \leq 0.05$, **$p \leq 0.01$, ***$p \leq 0.001$ (Student's *t*-test). (For interpretation of the references to color in this figure legend, the reader is referred to the Web version of this article.)

body weights were not significantly affected throughout the course of treatment (Supplementary Fig. 7D). In conclusion, our data demonstrate that combining SGK1 inhibitor and melatonin is effective in the treatment of cervical tumors through redox-modulating mechanism.

4. Discussion

Here we demonstrate that SGK1 is an antioxidative factor that promotes survival of cervical cancer cells and that inhibition of SGK1 confers vulnerability to redox dysregulation. Our study reveals a mechanistic basis by which SGK1 up-regulates antioxidant capacity to prevent elevation of ROS levels from exceeding the lethal threshold. We show that SGK1 activation induces the expression of NRF2 in a c-JUN-dependent manner. Combination of SGK1 inhibition and the pro-oxidant action of melatonin promotes ROS over-accumulation and enhance cervical cancer cell cytotoxicity.

SGK1 has long been known as a survival factor in response to various types of cellular stress stimuli including oxidative stress [46]. Lack of Sgk1 activity in mouse decidualizing cells enhances susceptibility to oxidative stress-induced apoptosis [47]. SGK1 protects endothelial cells against oxidative stress and apoptosis induced by hyperglycaemia [48]. While several studies have suggested the effects of SGK kinases, especially SGK1, on redox homeostasis in pathological settings [17,20], prior data linking SGK1-mediated redox modulation to the development of cancer is sparse [24]. In the current study, we investigated the molecular mechanism underlying the cytotoxic effect of SGK1 knockdown on cervical cancer cells. Indeed, our GSEA analysis of RNA-Seq data followed by functional assays in cervical cancer cell lines uncovered an antioxidative role of SGK1 through modulation of NRF2 expression. In strong support of our findings, analyses of gene expression datasets from human cervical cancer cohorts revealed significant association between the expression of SGK1 and NRF2 as well as the transcriptional signature involving NRF2. These data corroborated our findings that SGK1 engages redox homeostasis through induction of NRF2 expression and activity.

NRF2 is one of the master regulators of cellular antioxidant response and ROS homeostasis [6,8,49]. NRF2 activation may arise from diminished NRF2 turnover tightly regulated by its negative regulator KEAP1 [36,50]. Recent TCGA analysis reveals that *NRF2* is recurrently mutated in up to 7% of human cervical cancers [14,15]. Interestingly, majority of the mutations are localized in the domain of NRF2 protein critical for the interaction with KEAP1, suggesting the involvement of aberrant activation of NRF2 signaling in disease pathogenesis and therefore a therapeutic opportunity. Alternatively, NRF2 activation may also arise from increased *NRF2* transcription [36,51]. The c-JUN transcription factor binds to a specific promoter sequence in the *NRF2* gene and transcriptionally regulates *NRF2* expression [36,52]. Meanwhile, SGK1 has been shown to promote the differentiation of T_H1 and T_H2 differentiation through enhancing the stability of JUNB protein [40], another member of the JUN transcription factor family [41]. Given these previous findings, we considered the possibility that SGK1 induces NRF2 expression via JUN transcription factors. Indeed, we found that SGK1-activated cervical cancer cells are dependent on c-JUN but not on JUNB, and that knockdown of c-JUN abrogates the induction of NRF2 mRNA expression caused by SGK1 activation. Our work suggests the SGK1/c-JUN axis as a novel mechanism to elevate NRF2 expression and activity in cervical cancer cells (Fig. 7).

Melatonin, a powerful scavenger for free radicals, has been shown to display antiproliferative effects through inducing an antioxidant environment [42]. However, increasing evidence has pointed to the pro-oxidant activity of melatonin in association with its cytotoxic effects on several types of cancer [42,43,53]. In agreement with these studies, we find that melatonin, when present at mM ranges, promotes ROS production and induces cytotoxicity in cervical cancer cells. Moreover, we show that activation of the antioxidative factor SGK1 alleviates the cytotoxic effect of melatonin. Indeed, several lines of evidence have reported the potentiating effects of melatonin on chemotherapy-induced cytotoxicity in tumor cells [42]. For example, melatonin has been shown to enhance the sensitivity of HeLa cervical cancer cells to cisplatin *in vitro* due to ROS overproduction [54]. In the current study, we demonstrate that melatonin potentiates the cytotoxic effects of SGK1 inhibition in cervical cancer cells both *in vitro* and *in vivo*, most likely through a redox-modulating mechanism. It is worth noting that our study does not exclude the possibility that mechanisms other than ROS over-accumulation may account for the superior therapeutic effect induced by melatonin and SGK1 inhibitor. Instead, our study provides new insights into the utility of melatonin as a powerful synergistic agent in the treatment of cervical cancer.

5. Conclusion

Our study highlights the role of SGK1 in promoting cervical cancer cell survival by an anti-ROS mechanism. Specifically, SGK1 induces *NRF2* expression and antioxidant activation in a c-JUN-dependent manner. Combining SGK1 inhibition and melatonin as a pro-oxidant results in ROS overproduction and enhances cytotoxicity in cervical cancer cells. Targeting the antioxidant SGK1-c-JUN-NRF2 axis may therefore represent an effective and promising therapeutic strategy against cervical cancer.

Authors' contributions

H.C., P.L., M.W., and J.W. conceived and designed the study, and wrote the manuscript. M.W., Y.X., and L.S. performed major experiments, collected, and analyzed data. M.W., Y.X., and X.S. performed flow cytometric analysis. M.W., L.S., and J.Y. performed quantitative RT-PCR analysis and IHC staining. Z.T. conducted GSEA analysis. P.Q. conducted clinical data analysis. All authors contributed and approved the manuscript.

Funding

This work was supported by the National Natural Science Foundation of China (No.81472447, No. 81672575 and No. 81874111 to H Cheng; No. 81572586and No. 81372853 to P Liu; No. 81602309 to J Wang), the Liaoning Provincial Climbing Scholars Supporting Program of China (H Cheng, P Liu), and the Liaoning Provincial Key Basic Research Program for Colleges and Universities (LZ2017002 to H Cheng).

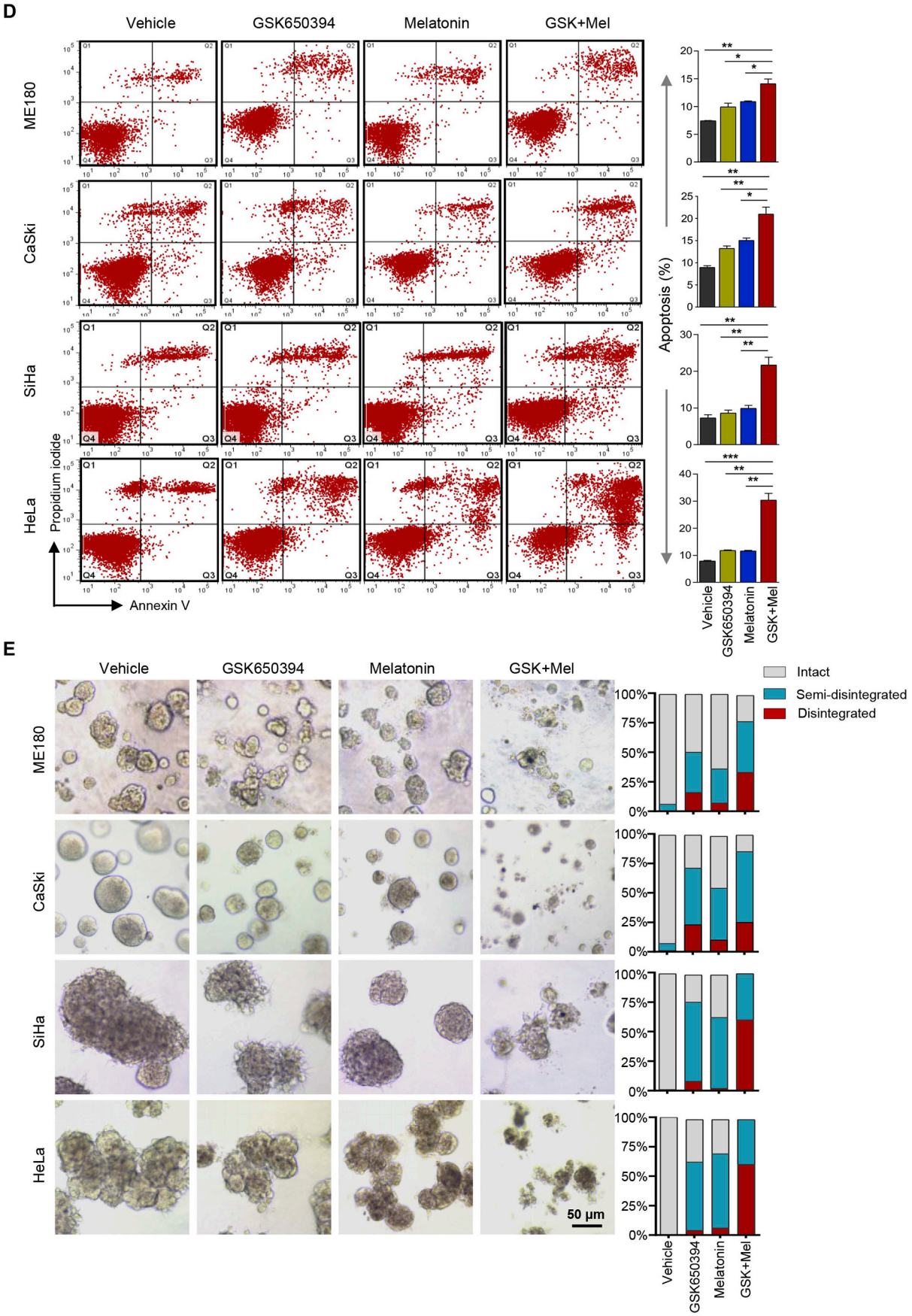

Fig. 5. (*continued*)

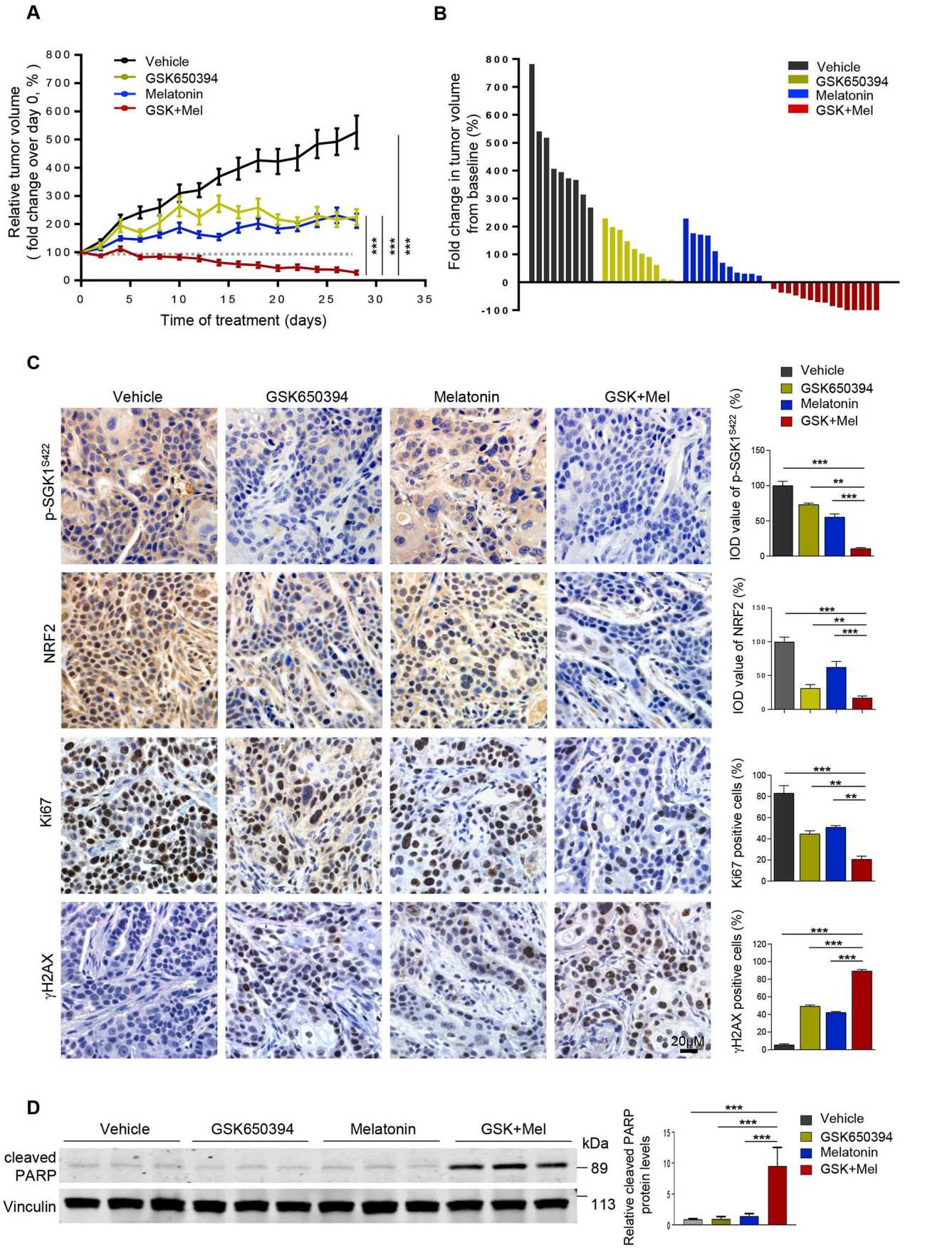

(caption on next page)

Fig. 6. Combined use of SGK1 inhibitor and melatonin is effective *in vivo*. (A) ME180-xenografted mice were treated with GSK650394 (10 mM, 40 μl/day, subcutaneous administration) or melatonin (50 mg/kg/day, intraperitoneal administration) alone, or in combination. The graph shows the fold change in tumor volume, with respect to the initial treatment at day 0. Vehicle, n = 9; GSK650394, n = 10; melatonin, n = 11; the combination, n = 15. ***P < 0.001 by a one-way ANOVA, with Tukey's multiple comparison tests. The data are shown as the mean ± S.E.M. (B) The waterfall plot indicates fold changes in tumor volume in mice treated as indicated. Fold changes were calculated by (endpoint tumor volume-baseline)/baseline. Note: baseline (tumor volume on Day 0). (C) Representative images of immunohistochemical staining for proteins in ME180-xenograft tumors treated as in (A) for 4 days. The data are shown as the mean ± S.E.M. IOD, integrated optical density. Scale bars, 20 μm. (D) Western blot analysis of cleaved PARP in tumor lysates from mice treated as indicated. Vinculin was used as a loading control. The quantification of protein abundance is shown. **p ≤ 0.01, ***p ≤ 0.001 (Student's *t*-test).

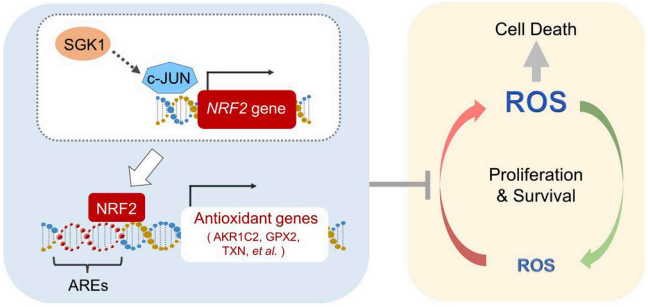

Fig. 7. Proposed model of the antioxidant axis SGK1-c-JUN-NRF2 in cervical cancer. SGK1 is an anti-oxidative factor that regulates survival of cervical cancer cells. Mechanistically, SGK1 induces the expression of redox-sensitive transcription factor NRF2 in a c-JUN dependent manner, which leads to the increased transcriptional expression of antioxidant genes that contain AREs. Inhibition of SGK1 can be exploited as a cancer vulnerability to redox dysregulation. Combinations of SGK1 inhibitors and ROS-generating agents, such as melatonin for its pro-oxidant action, could be a potent therapeutic strategy to promote ROS accumulation over the cell-death threshold and selectively kill cervical cancer cells. AREs, Antioxidant Response Elements.

Declarations of interest

None.

Acknowledgments

We thank members of Dalian Key Laboratory of Molecular Targeted Caner Therapy and the Liu Laboratory for discussions throughout the study.

Appendix A. Supplementary data

Supplementary data to this article can be found online at https://doi.org/10.1016/j.redox.2019.101225.

References

[1] L.A. Torre, F. Bray, R.L. Siegel, J. Ferlay, J. Lortet-Tieulent, A. Jemal, Global cancer statistics, 2012, Ca - Cancer J. Clin. 65 (2015) 87–108.
[2] F. Bray, J. Ferlay, I. Soerjomataram, R.L. Siegel, L.A. Torre, A. Jemal, Global cancer statistics 2018: GLOBOCAN estimates of incidence and mortality worldwide for 36 cancers in 185 countries, Ca - Cancer J. Clin. 68 (2018) 394–424.
[3] D. Trachootham, J. Alexandre, P. Huang, Targeting cancer cells by ROS-mediated mechanisms: a radical therapeutic approach? Nat. Rev. Drug Discov. 8 (2009) 579–591.
[4] C. Gorrini, I.S. Harris, T.W. Mak, Modulation of oxidative stress as an anticancer strategy, Nat. Rev. Drug Discov. 12 (2013) 931–947.
[5] M.B. Sporn, K.T. Liby, NRF2 and cancer: the good, the bad and the importance of context, Nat. Rev. Canc. 12 (2012) 564–571.
[6] M. Rojo de la Vega, E. Chapman, D.D. Zhang, NRF2 and the hallmarks of cancer, Cancer Cell 34 (2018) 21–43.
[7] S. Menegon, A. Columbano, S. Giordano, The dual roles of NRF2 in cancer, Trends Mol. Med. 22 (2016) 578–593.
[8] T. Suzuki, H. Motohashi, M. Yamamoto, Toward clinical application of the Keap1-Nrf2 pathway, Trends Pharmacol. Sci. 34 (2013) 340–346.
[9] A. Cuadrado, et al., Therapeutic targeting of the NRF2 and KEAP1 partnership in chronic diseases, Nat. Rev. Drug Discov. 18 (2019) 295–317.
[10] H.M. Leinonen, E. Kansanen, P. Polonen, M. Heinaniemi, A.L. Levonen, Role of the Keap1-Nrf2 pathway in cancer, Adv. Cancer Res. 122 (2014) 281–320.
[11] J.Q. Ma, H. Tuersun, S.J. Jiao, J.H. Zheng, J.B. Xiao, A. Hasim, Functional role of NRF2 in cervical carcinogenesis, PLoS One 10 (2015) e0133876.
[12] X. Ma, J. Zhang, S. Liu, Y. Huang, B. Chen, D. Wang, Nrf2 knockdown by shRNA inhibits tumor growth and increases efficacy of chemotherapy in cervical cancer, Cancer Chemother. Pharmacol. 69 (2012) 485–494.
[13] G. Kontostathi, et al., Cervical cancer cell line secretome highlights the roles of transforming growth factor-beta-induced protein ig-h3, peroxiredoxin-2, and NRF2 on cervical carcinogenesis, BioMed Res. Int. 2017 (2017) 4180703.
[14] A.I. Ojesina, et al., Landscape of genomic alterations in cervical carcinomas, Nature 506 (2014) 371–375.
[15] N. Cancer Genome Atlas Research, et al., Integrated genomic and molecular characterization of cervical cancer, Nature 543 (2017) 378–384.
[16] J.K. Schwarz, et al., Pathway-specific analysis of gene expression data identifies the PI3K/Akt pathway as a novel therapeutic target in cervical cancer, Clin. Cancer Res. 18 (2012) 1464–1471.
[17] D. Lauro, et al., Role of serum and glucocorticoid-inducible kinase (SGK)-1 in senescence: a novel molecular target against age-related diseases, Curr. Med. Chem. 22 (2015) 3765–3788.
[18] P. Castel, et al., PDK1-SGK1 signaling sustains AKT-independent mTORC1 activation and confers resistance to PI3Kalpha inhibition, Cancer Cell 30 (2016) 229–242.
[19] E.M. Sommer, H. Dry, D. Cross, S. Guichard, B.R. Davies, D.R. Alessi, Elevated SGK1 predicts resistance of breast cancer cells to Akt inhibitors, Biochem. J. 452 (2013) 499–508.
[20] A. Di Cristofano, SGK1: the dark side of PI3K signaling, Curr. Top. Dev. Biol. 123 (2017) 49–71.
[21] U.M. Fagerli, et al., Serum/glucocorticoid-regulated kinase 1 (SGK1) is a prominent target gene of the transcriptional response to cytokines in multiple myeloma and supports the growth of myeloma cells, Oncogene 30 (2011) 3198–3206.
[22] I. Shanmugam, G. Cheng, P.F. Terranova, J.B. Thrasher, C.P. Thomas, B. Li, Serum/glucocorticoid-induced protein kinase-1 facilitates androgen receptor-dependent cell survival, Cell Death Differ. 14 (2007) 2085–2094.
[23] A.B. Sherk, et al., Development of a small-molecule serum- and glucocorticoid-regulated kinase-1 antagonist and its evaluation as a prostate cancer therapeutic, Cancer Res. 68 (2008) 7475–7483.
[24] M.J. Kim, et al., Negative regulation of SEK1 signaling by serum- and glucocorticoid-inducible protein kinase 1, EMBO J. 26 (2007) 3075–3085.
[25] W. Wu, S. Chaudhuri, D.R. Brickley, D. Pang, T. Karrison, S.D. Conzen, Microarray analysis reveals glucocorticoid-regulated survival genes that are associated with inhibition of apoptosis in breast epithelial cells, Cancer Res. 64 (2004) 1757–1764.
[26] J. Zhu, et al., Knockdown of long non-coding RNA XIST inhibited doxorubicin resistance in colorectal cancer by upregulation of mir-124 and downregulation of SGK1, Cell. Physiol. Biochem. 51 (2018) 113–128.
[27] C. Zhang, et al., Glucocorticoid-mediated inhibition of chemotherapy in ovarian carcinomas, Int. J. Oncol. 28 (2006) 551–558.
[28] K. Wang, et al., SGK1-dependent intestinal tumor growth in APC-deficient mice, Cell. Physiol. Biochem. 25 (2010) 271–278.
[29] J. Qin, J.X. Chen, Z. Zhu, J.A. Teng, Genistein inhibits human colorectal cancer growth and suppresses miR-95, Akt and SGK1, Cell. Physiol. Biochem. 35 (2015) 2069–2077.
[30] X. Liang, et al., Therapeutic inhibition of SGK1 suppresses colorectal cancer, Exp. Mol. Med. 49 (2017) e399.
[31] L.Y.W. Lee, et al., Serum- and glucocorticoid-induced kinase Sgk1 directly promotes the differentiation of colorectal cancer cells and restrains metastasis, Clin. Cancer Res. 25 (2019) 629–640.
[32] J. Ding, et al., Inhibition of BTF3 sensitizes luminal breast cancer cells to PI3Kalpha inhibition through the transcriptional regulation of ERalpha, Cancer Lett. 440–441 (2019) 54–63.
[33] D. Wang, et al., Effective use of PI3K inhibitor BKM120 and PARP inhibitor Olaparib to treat PIK3CA mutant ovarian cancer, Oncotarget 7 (2016) 13153–13166.
[34] C. Halle, et al., Hypoxia-induced gene expression in chemoradioresistant cervical cancer revealed by dynamic contrast-enhanced MRI, Cancer Res. 72 (2012) 5285–5295.
[35] F. Braso-Maristany, et al., PIM1 kinase regulates cell death, tumor growth and chemotherapy response in triple-negative breast cancer, Nat. Med. 22 (2016) 1303–1313.
[36] G.M. DeNicola, et al., Oncogene-induced Nrf2 transcription promotes ROS detoxification and tumorigenesis, Nature 475 (2011) 106–109.
[37] J. Park, M.L. Leong, P. Buse, A.C. Maiyar, G.L. Firestone, B.A. Hemmings, Serum and glucocorticoid-inducible kinase (SGK) is a target of the PI 3-kinase-stimulated signaling pathway, EMBO J. 18 (1999) 3024–3033.
[38] A.W. Wyatt, et al., DOCA-induced phosphorylation of glycogen synthase kinase 3beta, Cell. Physiol. Biochem. : Int. J. Exp. Cell. Physiol. Biochem. Pharmacol. 17 (2006) 137–144.
[39] Y. Yao, et al., Lnc-SGK1 induced by Helicobacter pylori infection and highsalt diet

promote Th2 and Th17 differentiation in human gastric cancer by SGK1/Jun B signaling, Oncotarget 7 (2016) 20549–20560.
[40] E.B. Heikamp, et al., The AGC kinase SGK1 regulates TH1 and TH2 differentiation downstream of the mTORC2 complex, Nat. Immunol. 15 (2014) 457–464.
[41] E. Shaulian, M. Karin, AP-1 as a regulator of cell life and death, Nat. Cell Biol. 4 (2002) E131–E136.
[42] H.M. Zhang, Y. Zhang, Melatonin: a well-documented antioxidant with conditional pro-oxidant actions, J. Pineal Res. 57 (2014) 131–146.
[43] I. Bejarano, J. Espino, C. Barriga, R.J. Reiter, J.A. Pariente, A.B. Rodriguez, Pro-oxidant effect of melatonin in tumour leucocytes: relation with its cytotoxic and pro-apoptotic effects, Basic Clin. Pharmacol. Toxicol. 108 (2011) 14–20.
[44] H.M. Zhang, Y. Zhang, B.X. Zhang, The role of mitochondrial complex III in melatonin-induced ROS production in cultured mesangial cells, J. Pineal Res. 50 (2011) 78–82.
[45] T. Muranen, et al., Inhibition of PI3K/mTOR leads to adaptive resistance in matrix-attached cancer cells, Cancer Cell 21 (2012) 227–239.
[46] M.L. Leong, A.C. Maiyar, B. Kim, B.A. O'Keeffe, G.L. Firestone, Expression of the serum- and glucocorticoid-inducible protein kinase, Sgk, is a cell survival response to multiple types of environmental stress stimuli in mammary epithelial cells, J. Biol. Chem. 278 (2003) 5871–5882.
[47] M.S. Salker, et al., Deregulation of the serum- and glucocorticoid-inducible kinase SGK1 in the endometrium causes reproductive failure, Nat. Med. 17 (2011) 1509–1513.
[48] F. Ferrelli, et al., Serum glucocorticoid inducible kinase (SGK)-1 protects endothelial cells against oxidative stress and apoptosis induced by hyperglycaemia, Acta Diabetol. 52 (2015) 55–64.
[49] C.E. Hochmuth, B. Biteau, D. Bohmann, H. Jasper, Redox regulation by Keap1 and Nrf2 controls intestinal stem cell proliferation in Drosophila, Cell Stem Cell 8 (2011) 188–199.
[50] M. Yamamoto, T.W. Kensler, H. Motohashi, The KEAP1-NRF2 system: a thiol-based sensor-effector apparatus for maintaining redox homeostasis, Physiol. Rev. 98 (2018) 1169–1203.
[51] M.K. Kwak, K. Itoh, M. Yamamoto, T.W. Kensler, Enhanced expression of the transcription factor Nrf2 by cancer chemopreventive agents: role of antioxidant response element-like sequences in the nrf2 promoter, Mol. Cell. Biol. 22 (2002) 2883–2892.
[52] S. Tao, et al., Oncogenic KRAS confers chemoresistance by upregulating NRF2, Cancer Res. 74 (2014) 7430–7441.
[53] A.M. Sanchez-Sanchez, et al., Intracellular redox state as determinant for melatonin antiproliferative vs cytotoxic effects in cancer cells, Free Radic. Res. 45 (2011) 1333–1341.
[54] R. Pariente, J.A. Pariente, A.B. Rodriguez, J. Espino, Melatonin sensitizes human cervical cancer HeLa cells to cisplatin-induced cytotoxicity and apoptosis: effects on oxidative stress and DNA fragmentation, J. Pineal Res. 60 (2016) 55–64.